DYNAMICS OF IMPINGING JETS
STUDIED IN TRANSVERSAL CROSS SECTION

Václav Tesař / Václav Něnička
Institute of Thermomechanics v.v.i., Academy of Sciences of the Czech Republic, Prague

Abstract

Authors investigated experimentally an air jet at $Re = 10\ 200$ *impinging on a flat plate positioned at* $h_S/D = 2.5$. *The object of interest were vortical instability structures that form in the outer, mixing-layer part of the jet. Their formation was triggered by azimuthal waves generated in the nozzle exit by a set of* 8 *actuators driven by suitably phase-shifted harmonic excitation signal at three different multiples of expected natural frequency. The structures were visualised by addition of water mist and by laser-light illumination in a plane perpendicular to the nozzle axis. The light formed a planar sheet at* $h_p/D = 1.875$, *illuminating a cross section that was photographed by a high-frequency camera located behind the impingement plate, which was transparent. Images of scattered light intensity were taken at a* 10 $\deg$ *phase intervals (i.e. taking* 36 *images per excitation period).*

1. Introduction

Impinging jets are of particular importance for heating and cooling - as well as for mass transfer applications - since they make possible achieving the highest transfer rates between a fluid and a solid surface (e.g., Tesař and Trávníček [1]). They are strongly influenced by presence of instability structures, of vortical character, which form in the outer, mixing-layer part of the jet – Tesař [3], Tesař and Barker [15]. The structures are considered to be responsible, e.g., for the off-axis transfer maxima, until recently enigmatic - Tesař [13]. Initially, the structures are regu-
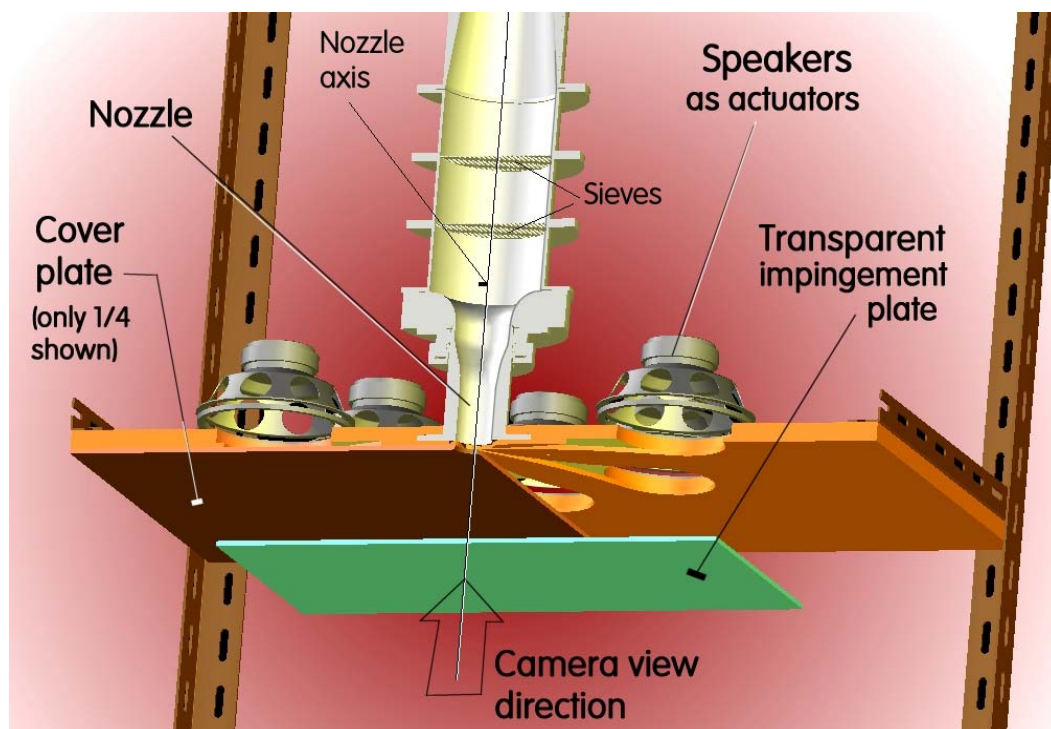

Fig. 1 Experimental rig, shown in section by vertical plane passing through the axis. A part of the cover plate is further removed to show the waveguides leading from the loudspeakers towards the nozzle exit.

lar and of coherent character, but they tend to decompose rather fast, Fig. 2, into what is in effect a chaotic turbulence. This immersion in - and interaction with - the stochastic vortices makes the study of the structures difficult. In the present investigations, they were studied by means of flow visualisation, using a laser-light sheet making effectively a section through the flow. The light photographed by a camera was due to scattering on water droplets, which were added to the air before it entered the blower that generated the air flow through the nozzle.

The main difficulty in studies of the vortical structures is the irregularity of their appearance. This problem was solved — as already described in earlier publications by Tesař and Něnička, [8] and Tesař, Něnička, and Šonský [7] — by triggering the structure formation by a weak excitation in the nozzle exit. As seen in Fig. 1, the nozzle is surrounded by eight actuators driven by suitably phase-shifted harmonic excitation signal so that they produce in the nozzle exit an azimuthal wave (in fact, two such waves, chasing one another). It should be emphasised that the waves do not **generate** the studied structures, which would be produced even without such excitation due to the inherent hydrodynamic instability. What the excitation achieved was triggering the vortex formation at precise instants of time. The triggering was synchronised with the picture taking by the camera. As a result, in a set of images obtained at the same phase of the excitation signal, the different vortical structures are mutually very similar, especially at an early stage of their development, so that they make an appearance of a single structure "frozen" in space. This makes possible evaluating e.g. the phase averaged motions in the fluid. These are the basis upon which the chaotic motions was superimposed.

The ultimate target of the planned investigations - not discussed in the present paper - are the paradoxical spectral transport properties of helical instability structures (Moiseev et al. [19], Moiseev and Pungin [20]). We believe this energy transfer to the larger scales is an effect taking place during an interaction of two helical structures. It was with this idea in mind that the actuators were designed to actually contain twice as many loudspeakers (eight rather than four) that are in principle necessary for producing a smooth azimuthal wave. As mentioned above, with the two waves it is possible to generate two helical structures running one after another along the circumference of the nozzle exit.

Equally as in similar earlier investigations by the present authors, e.g. as described in the references [8] and [9], the jet was generated in a rig with the nozzle of exit diameter $D = 40$ mm. The exit of this nozzle was located in the centre of a large (890 mm x 890 mm) plate perpendicular to the jet axis, as shown Fig. 4. Aerodynamic properties of this nozzle were published earlier in [14]. Some previous investigations studies unbounded jets, but in the present case the jet, after leaving the nozzle, impinged on a flat plate. This was held at a fixed
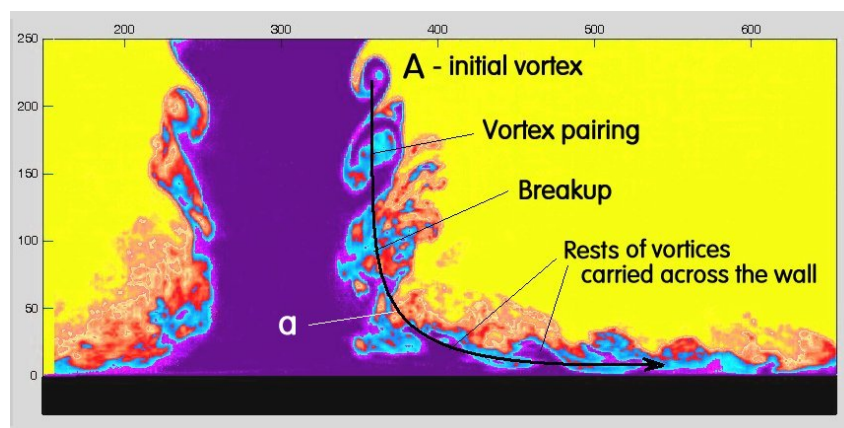

Fig. 2 Typical example of visualised impinging jet at a Reynolds number ($Re = 10.2\ 10^3$), typical for heat transfer applications, seen in meridian plane section. The relative height of the nozzle $h_S/D = 2.5$, excitation frequency at Strouhal number $Sh = 2.3$. During their motion towards the impingement wall, roughly along the trajectory a, the vortical structures in the mixing layer gradually decompose – by the succession of vortex pairing and break-up — the process finally leading to chaotic turbulence.

position, such that the nozzle exit was at relatively small height h_S, above the plate, the relative distance (related to the nozzle exit diameter) being $h_S/D = 2.5$. In the previous investigations discussed in [8] and [9], the laser light sheet illuminated the jet in a meridian plane, i.e. a vertical plane containing the jet axis. On the other hand, the attention in the present paper focuses on the more recent studies with transversal laser-light cross-section through the jet. The impingement plate was transparent (made of glass) — Fig. 1 — and the camera was positioned below it, looking towards the nozzle exit. Due to various constraints (such as the limited available space between the impingement plate below and the actuator plate above for the laser, which was to be placed near to the nozzle because the used high-speed camera required a rather high illumination power), the light sheet was very near to the nozzle exit. Its relative axial distance from the nozzle was only $0.625\ D$. At this distance the meridian plane sections in the earlier investigations have shown a relatively well ordered character of the observed vortical structures. It was therefore hoped that also the shapes seen in the transversal sections will be rather simple and regular - and provide an explanation for some of the previously observed features.

2. Triggering and image processing

Of course, the weak triggering could be expected to be successful only if the excitation frequency corresponded to the natural frequency with which the instability structures appear. Its evaluation is not easy and exhibits a considerable scatter because of the irregularity of their appearance. Information available at that stage concerning the natural frequency is presented in Fig. 3, in the form of Strouhal number Sh on Reynolds number Re. It is based on data from references [10], [17], and [18] and also upon the values evaluated by the present first author (Tesař, 2005) from flow visualisation data obtained by Regunath [4]. While the frequency – from which the Strouhal number is evaluated – was measured by authors of [10], [17], and [18] directly, no suitable instrumentation was available to the present authors and they computed the frequency indirectly, from the position of the vortices in the images. To evaluate from them the frequency, it is necessary to know the convection velocity with which the vortices were carried
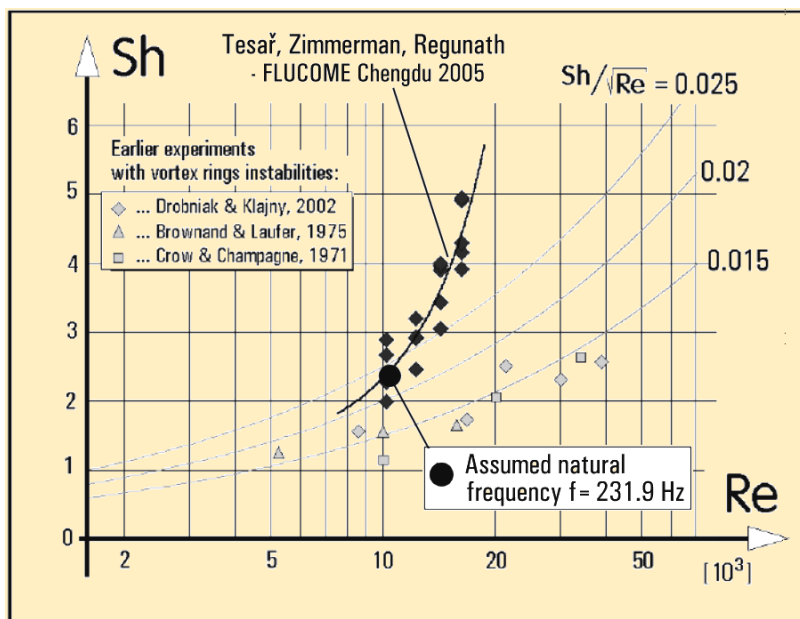
Fig. 3 Dependence of Strouhal number Sh of the naturally appearing vortical structure on the Reynolds number Re of the flow through the nozzle — as it was evaluated from earlier jet flow visualisation images [4] using the nozzle exit velocity as the characteristic velocity for evaluation of the Strouhal number Sh. The operating point was chosen to be at the location indicated by the large round dot.

with the jet. No access to reliable data about the convection of vortices was available, however, and the value therefore used as the characteristic velocity was the magnitude of the computed velocity in the nozzle exit. This was later found to be a mistake. An indication that something is wrong is apparent from the disagreement in Fig. 3. There are reasons (based on the Reynolds number dependence of the growth of the laminar mixing layer) for an expectation that the data in Fig. 3 should follow the curve of constant value of the ratio $Sh/\sqrt{Re}$.

Unfortunately, the results of the present first author's experiments described in [4] are seen in Fig. 3 to deviate considerably from this expected dependence, especially at higher Reynolds numbers. It was decided for the experiments discussed in the present paper to chose the value of Reynolds number $Re = 10.2\ 10^3$ – this is a location at which the deviations between the data from 2005 and the results of other researchers did not seem to be as large as at higher Re and yet the Reynolds number was high enough to expect presence of substantial turbulence. The excitation frequency corresponding to the vertical location $Sh = 2.3$ of the chosen operation point. This corresponds to the value of the natural frequency $f = 231.9$ Hz. Because the actuators were designed, as already mentioned above, to generate two azimuthal waves, one after another, in the nozzle exit, the value actually adjusted for driving the actuators of the triggering system was $f = 115.9$ Hz, i.e., one half of the value indicated in Fig. 3.

The values of the scattered light intensity recorded by the camera Vision Research Phantom v7.3, with 14-bit monochrome SR-CMOS sensors, giving 800 x 600 pixels resolution and offering maximum top speed of 6 688 frames per second. The 14 bit resolution means theoretical range of recorded grey scale values from 0 to 16 384, but in practical situations the values stored at a particular pixel location were in a more narrow range. The value for the black colour of the outer air should be theoretically 0, as it contains no light-scattering water droplets prior to its entrainment into the jet. In reality there is, however, always some inevitable other scattering (e.g., due to dust in the air) inside the test space and also the absorbance of the background (which was black textile) is never perfect. On the other hand, the camera sensitivity was to be traded off for the recording. The output from the camera was downloaded in the form of a matrix with rows and columns corresponding to those of the camera pixels. The first step in their processing was renormalisations to the 0 − 255 (8bit) range, more suitable for further data processing. Then, also to make their subsequent processing faster, the size of the matrices was reduced, whenever possible, by deleting the outer parts of the camera view field whenever this did not show objects of possible interest.
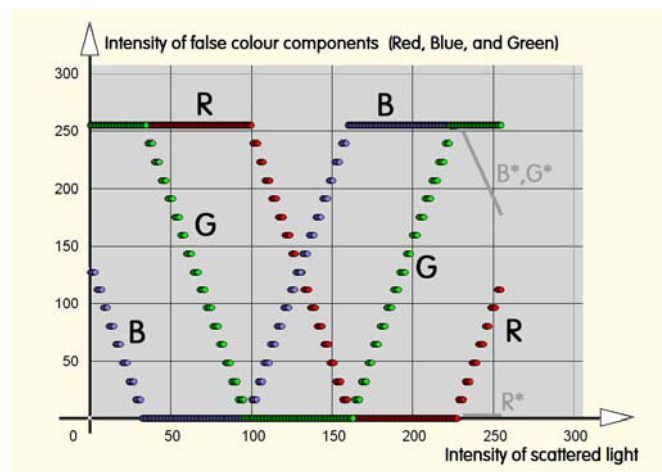

Fig. 4 An example of transformation function successfully used for conversion recorded intensities of scattered laser light into the false-colour image. For symmetry of the function, the red component R here rises at the blue end of the colourbar while B and G remain high. This makes the jet core appearing somewhat too bright, better appearance may be obtained with the suggested alternative marked with asterisks.
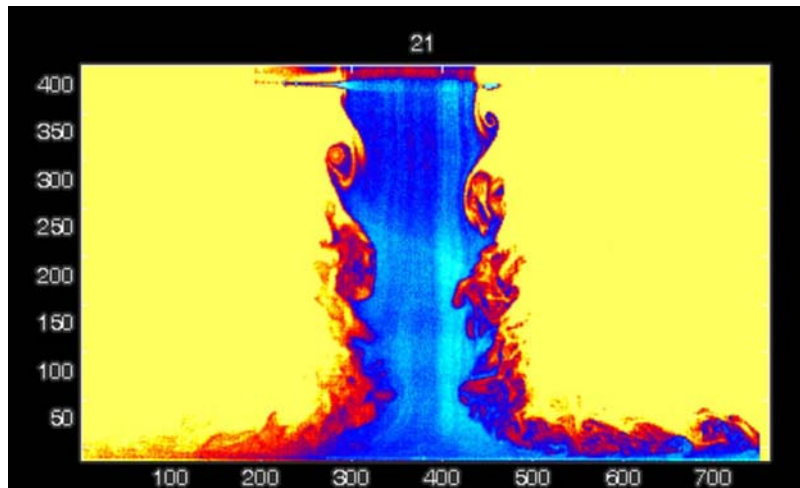
Fig. 5 An example of false colour image of an impinging jet. Numbers in the boundary regions indicate the indexes of the matrix elements that store the pictorial information.

To make the variations of the recorded intensity values more apparent, it was found useful to transform, in the next step, the grey-scale into a range of false colours. It is interesting how this colouration can make visual inspection of the resultant colour images much more effective. Of many possible false-colour transformation functions, the one that was found particularly suitable is presented in diagrammatic form in Fig. 4. The following Fig. 5 then present an example of the image of the impinging jet – here photographed in meridian-plane slice – that was processed this way. The background (with absence of water mist droplets and hence low scattered light intensity) appears yellow. The most important outer mixing layer of the jet, with prominent vortices, is presented at various intensities of red. The core part of the jet (with maximum droplet concentration) is shown as blue. The colour of this core appears to be too bright and in Fig. 4 there is a suggested alternative of the transformation function slightly corrected at the high-intensity end (this was not applied in the example in Fig. 4). The corrected function would produce darker regions with high concentration of the scattering particles.

The main purpose behind the presentation of the example in Fig. 5 is demonstration of the helical character of the vortices observed in the mixing layer of the jet. The helicity is best seen in the following Fig. 6. This picture shows the same flowfield as Fig. 5, this time, however,
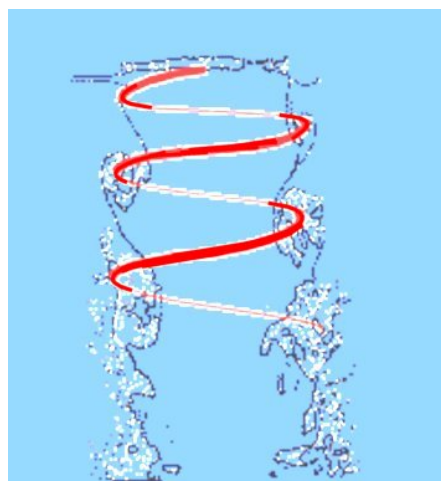

Fig. 6 Contours demarcating the boundaries between the areas evaluated by posterisation of the jet from Fig. 5 are shown here together with superimposed lines that indicate the core of the helical instability vortex structure.
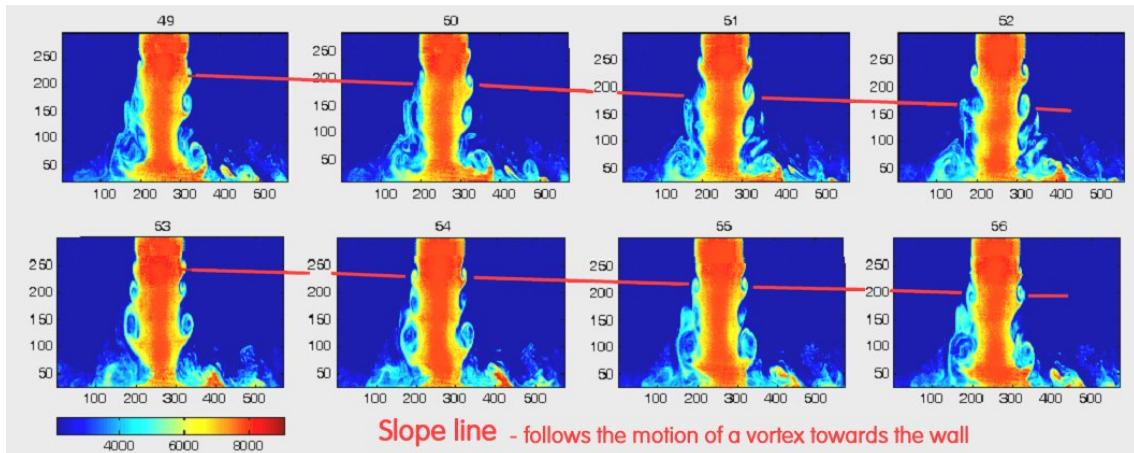
Fig. 7 Actual development and convective motion of a particular vortical structure photographed in a fast succession of time instants (in this case each frame differs from its neighbour by the phase increment 5 deg of full 360 deg circle) after the beginning of the triggering action. The sloping red line connects images of a particular vortex as it progresses towards the wall.

processed so as to show iso-concentration contours. These were evaluated as the boundaries (the demarcation lines) between the regions of posterised image [8]. In particular, these contour lines show in Fig. 6 very distinctly the positions of the vortex core at both (the left-hand as well as right-end) sides of the jet. The red sinusoidal line was then drawn so that its maximum amplitude positions coincided with these core location. The illustrations shows in a quite convincing manner that the vortical structure in the mixing layer does not consist of a series of vortex rings, but a single helical structure.

Further processing of the images was mostly done by handling multi-image sequences. There are two main ways how to select images to form the sequence – both are shown here on an example of the meridian plane sections in Figs. 7 and 8. It is useful to note the ordinal numbers written above each image in the sequence. In Fig. 7, there is a direct time dependence, with the images recorded one-by-one at a constant time increment steps. In this case, the se-
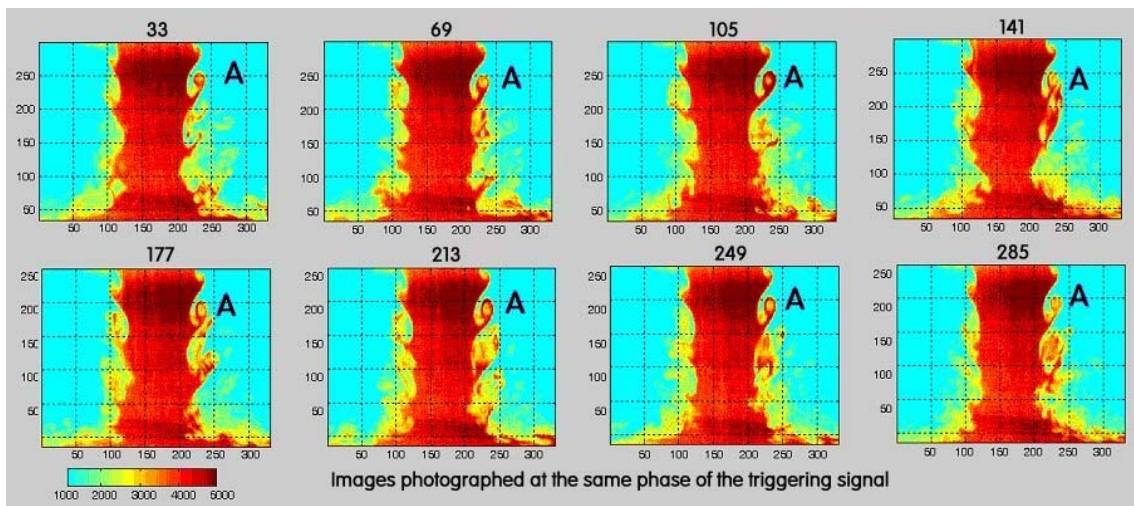
Fig. 8 Demonstrated effect of the synchronised picture taking. These impinging jet images were photographed at the same phase of the triggering azimuthal acoustic waves. Vortices – such as the one marked A - were, of course, generated at different instants of time (note the numbers that indicate the image ordinal number; the images are here separated by 10 deg steps in the 360 deg period). Because they are photographed in the identical phase of their development, the structures are in the same position and appear as if they were a single stationary object.
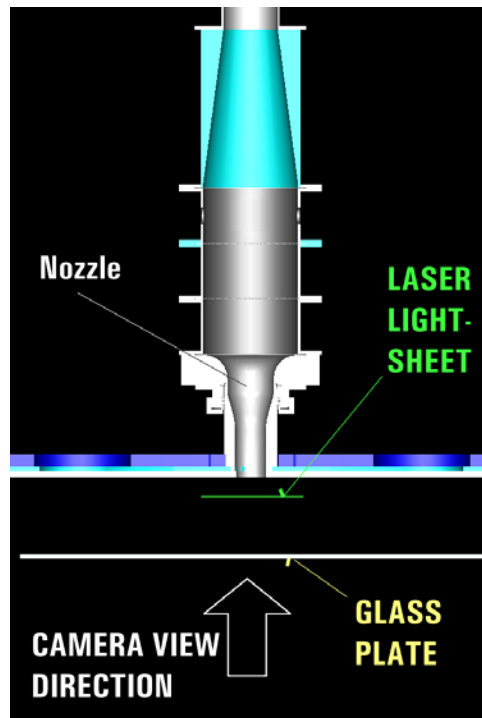
Fig. 9 A detail of the nozzle in the experimental facility (cf. Fig. 1) and of the space between the nozzle and the impingement plate. The picture shows the position of the laser light sheet plane (shown green – because this is the actual the colour of the used laser light).

quence is suitable for evaluation of the propagation speed of a particular structure. It is, however, difficult to evaluate the character of the changes caused by the vortex decomposition and transition into the chaotic movements because at each time instant the same vortical structure is found in different images at different spatial positions. On the other hand, the individual images in the other sequence presented in Fig. 8 are mutually separated by the full excitation period. This illustrations demonstrates the success of the triggering and of the picture taking synchronisation: at the initial stages, immediately downstream from the nozzle exit, the individual structures (such as those marked A) appear to be nearly identical – as if the images were showing the same structure. It is easy then to perform the phase averaging that reveals the common features of all the images of the sequence – and then to evaluate the deviations from this average.

3. The structures in cross-section views

The main objective of the discussed investigation was now to see the studies vortical structures in the transversal sections through the jet (rather than the longitudinal sections by the meridian plane, discussed so far in association with Figs. 2 to 8). The following Figs. 9 and 10 (together with Fig. 1 above) provide an information about the location of the light-"knife" relative to the jet-generating nozzle and the impingement plate. By comparison with, e.g., the example presented in Fig. 5, this section passes through the initial development stages of the jet where in the longitudinal section there are clearly recognisable instability vortices, with only minimal influencing by stochastic processes that dominate further below (cf. Fig. 2). It could be expected that also the transversal sections would show a similar degree of regularity. It was therefore quite disappointing that typical images – like the one presented here in Fig. 11 in the posterised version – have shown unexpected complexities. Of course, the complexity could be attributed to the chaotic turbulence.
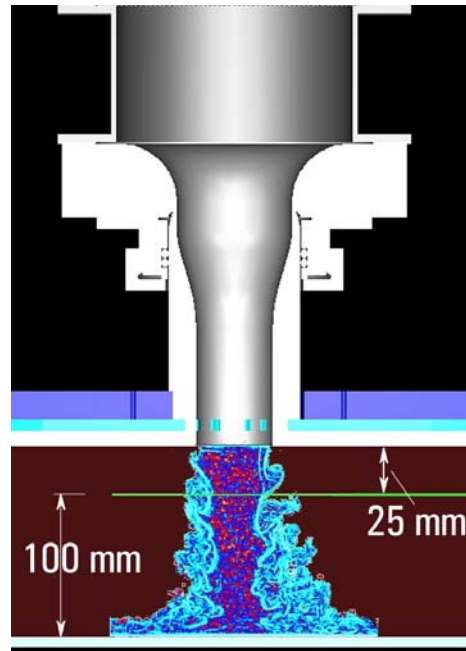
Fig. 10 Another, closer detail of the light sheet passing transversally through the jet. At the distance 25 mm downstream from the nozzle exit, this "section" plane passes through the potential core of the jet, surrounded by the annular shear region – the mixing layer (Tesař 2006). Small inserted picture of the jet was actually evaluated form a longitudinal-section photograph by computing and false-colouring the values of correlation coefficient [8].

As expected, nothing of importance takes place in the potential core of the jet. Important phenomena take place only in the annular outer layer, which corresponds to the mixing layer of the jet. Among the characteristic features found there by analysis of the transversal-section images, the most apparent were the redial "tentacles" reaching outwardly from the jet into the surrounding outer fluid and the regions of entrained outer fluid.

Two generic "tentacles" are in Fig. 11 indicated by the red arrows showing the radial direction of the jet fluid motion and (equally red) letter R.

The other immediately apparent feature in Fig. 11 (and other images) are the volumes filled by the outer fluid — which contains very few water-mist droplets and therefore is coloured white in the two-valued (white – blue) posterisation. Such entrainment of the outer fluid into the mixing layer was, of course, expected, but it was expected in the form of elongated "half-moon" shapes at nearly constant radius from the jet axis and long tangential or circumferential dimension. Instead, those observed (among others e.g. the ones marked in Fig. 11 as A, B, and C and coloured red and blue in the following sequence of images Fig. 12). exhibit only small elongation. They are, in fact, nearly circular. They are mutually separated by considerably thick regions of the inner, jet fluid (containing high concentration of the water mist droplets added to the air upstream from the blower). If the sequence of images from Fig. 12 is set up into a video clip, these "voids" are seen to move. Their motion is directed tangentially (not radially) and what is particularly surprising, the distances travelled are rather short. The sequence in Fig. 12 was included into this paper just to show this motion. The voids A, B, and C not only do not travel far during the period of the triggering excitation. They move a distance comparable with their dimension and then disappear. Even more surprising fact is the (tangential) direction of their movement is not the same - A and C (coloured blue) move anti-clockwise - while the (red coloured) B moves clockwise. This is shown in Fig. 13 wjwere the arrows indicating the motion direction were found by following in detail the sequence presented in Fig. 12.
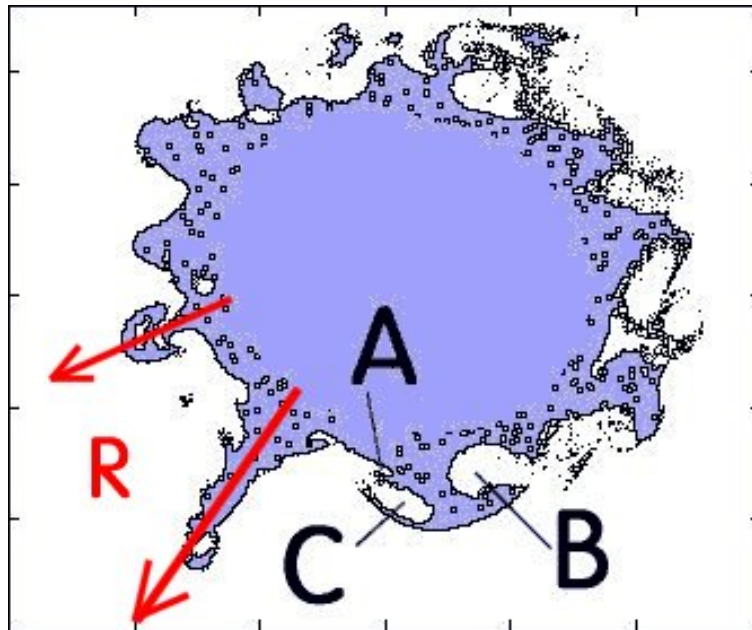
Fig. 11   Typical features of the jet cross section – seen here in the extreme posterisation – drasctic reduction of the colour palette to just single colours. The first apparent feature is the formation of radial "tentacles" R, their motion direction marked by the red arrows, which obviously transport the jet fluid radially outwards. The other feature are the large gaps containing the outer fluid (containing no water mist droplets). Three such gaps or voids are here marked A, B, and C so that their behaviour through one period (i.e. in the sequence of the type shown above in Fig. 7) may be followed in Fig. 12.
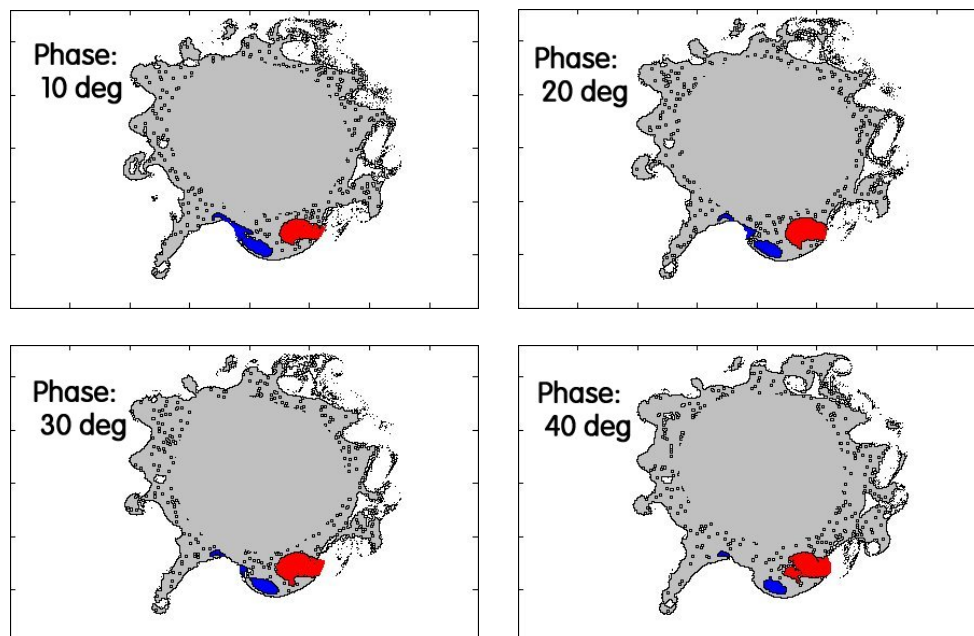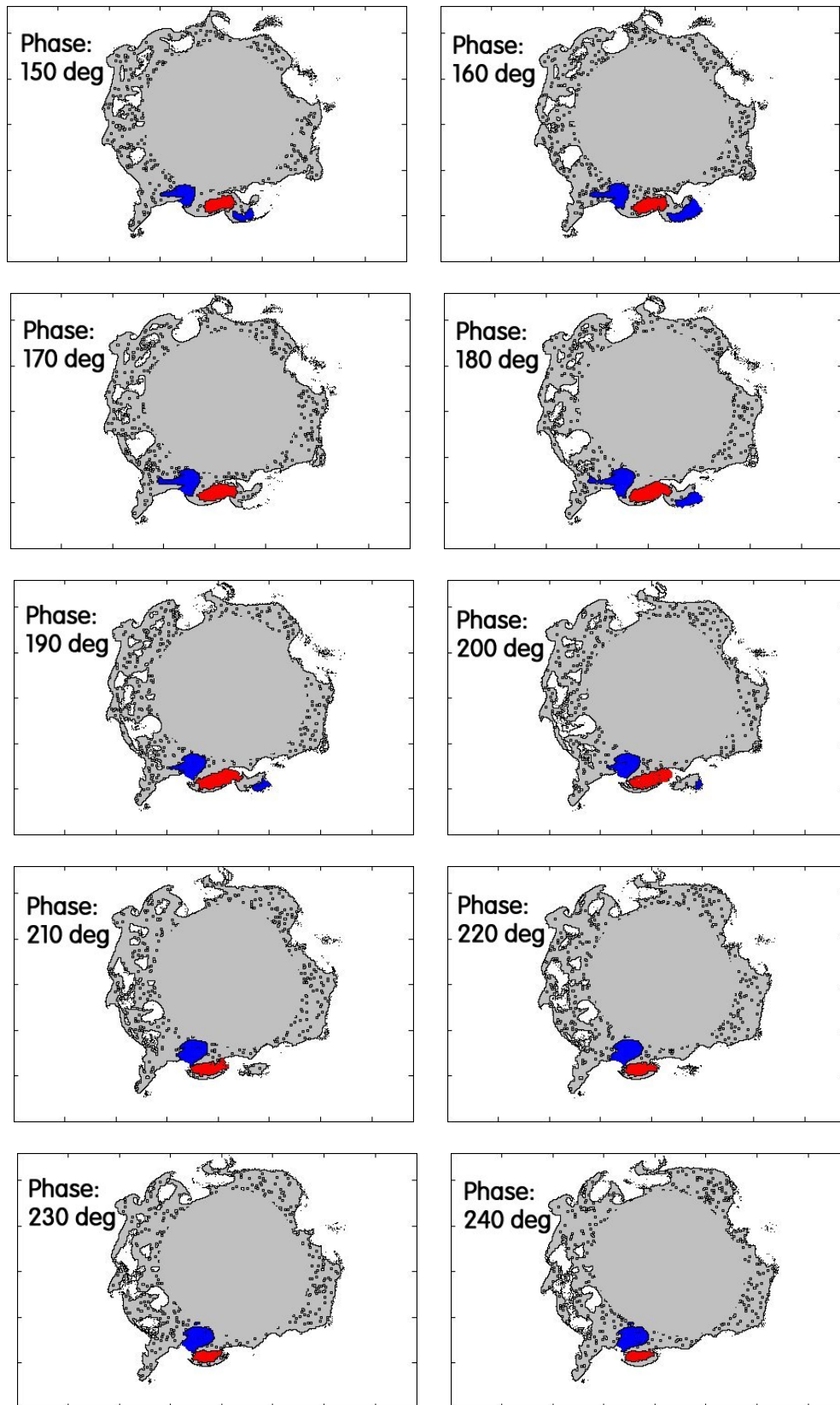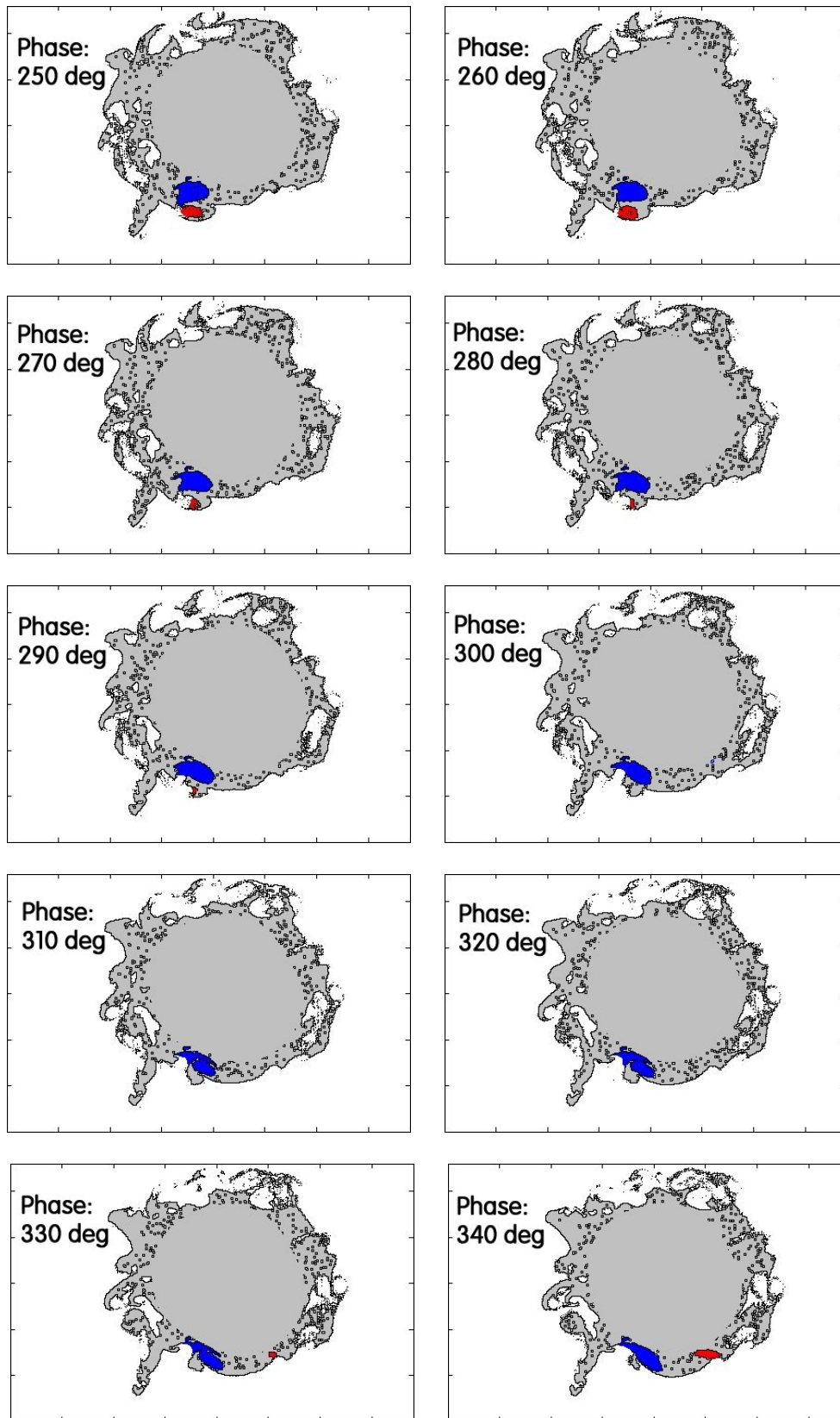

Fig. 12 – Continued on the next page
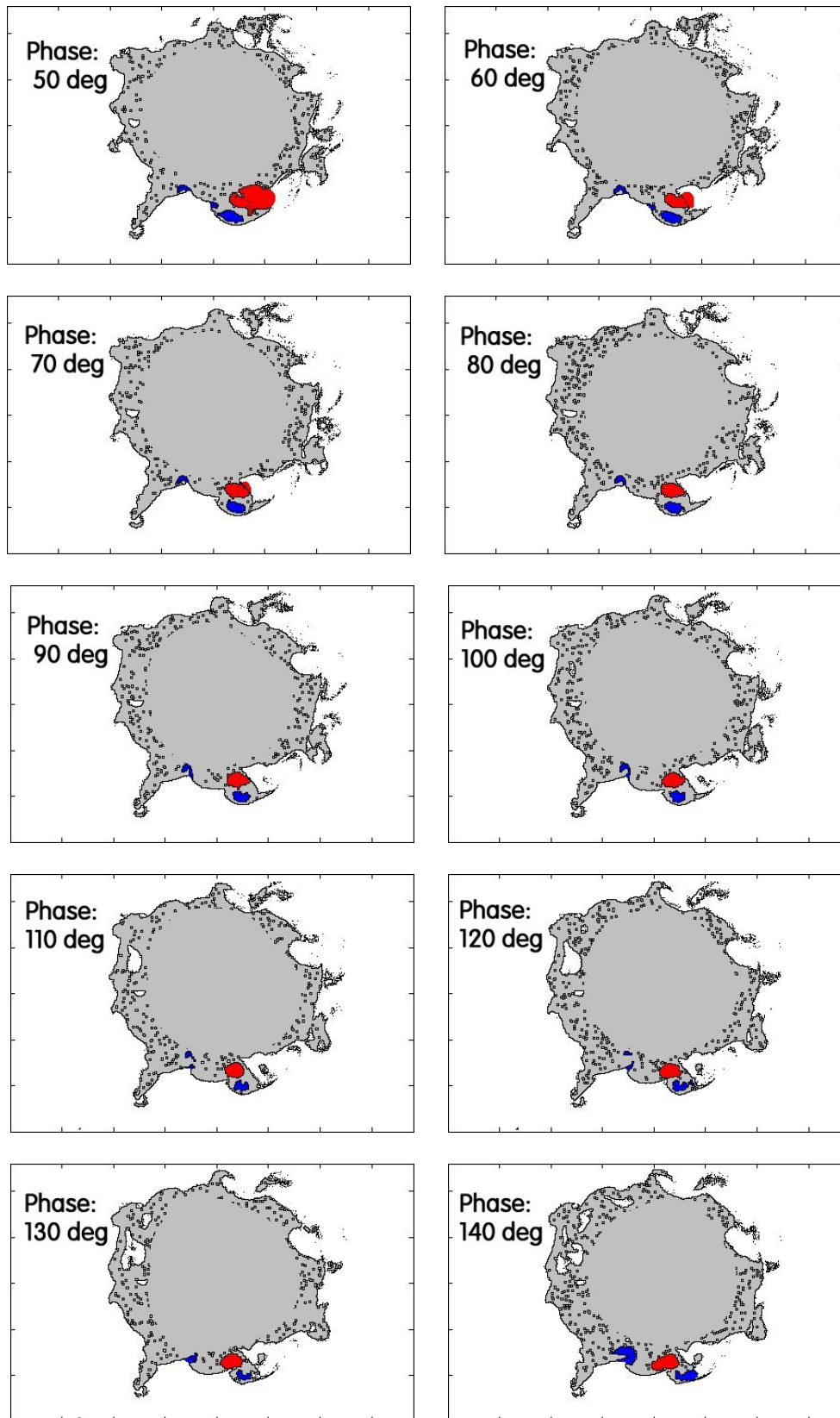
Fig. 12 – Continued on the next page

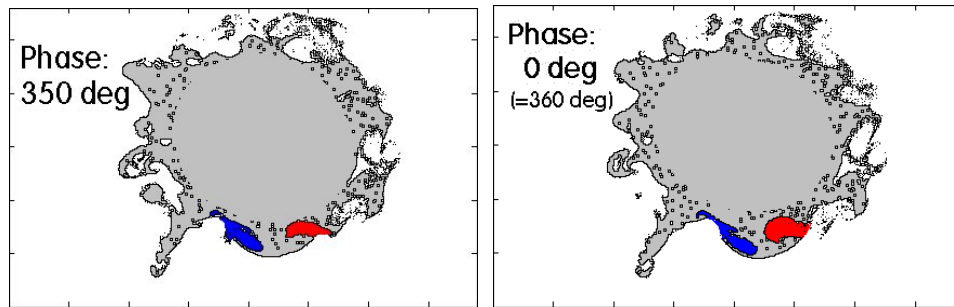Fig. 12 – Continued on the next page

Fig. 12 – Continued on the next page

Fig. 12 Sequence of posterised cross-section images (there are 36 images photographed at phase increment 10 deg out of the full 360 deg period) showing the motions of the coloured large gaps A, B, and C in the course of the excitation period – excitation frequency f = 115.9 Hz, i.e., one half of the value indicated in Fig. 3. There is admittedly a large number of images in this sequence, covering the whole excitation period, but this was considered necessary to enable any reader to study the motion details.
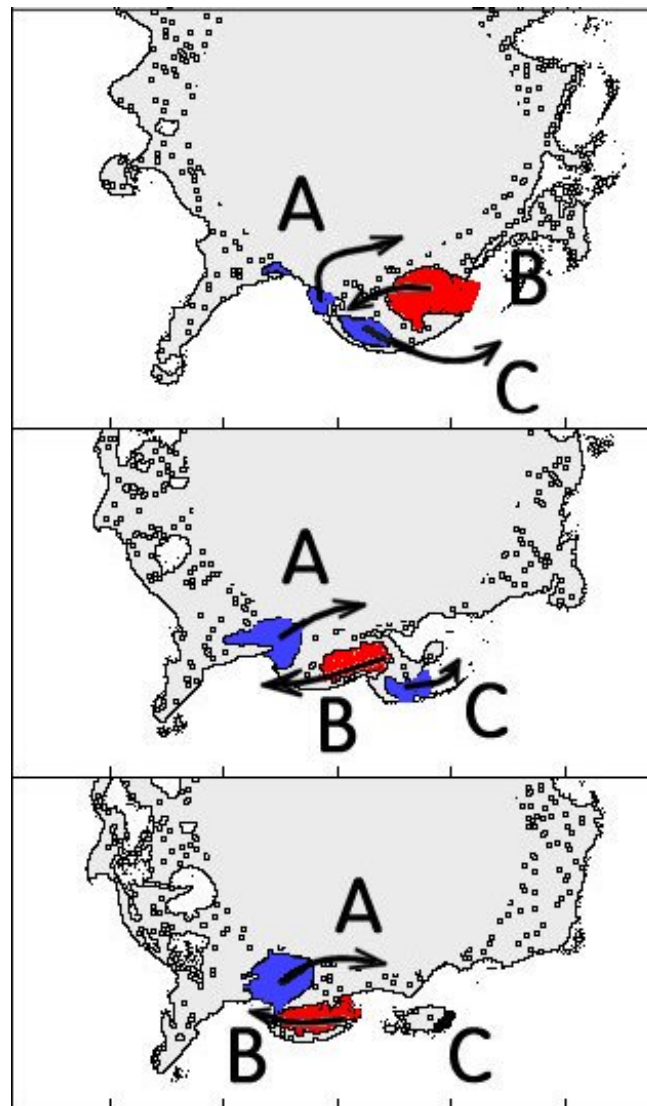

Fig. 13 Character of the movement of the three selected coloured large gaps A, B, and C. The two that are coloured blue (A and C) move to the right-hand side – while the red coloured one (B) moves between A and C to the right. At the end of their travel the voids disappear (which is what is here seen to happen to the void C in the lowest image.
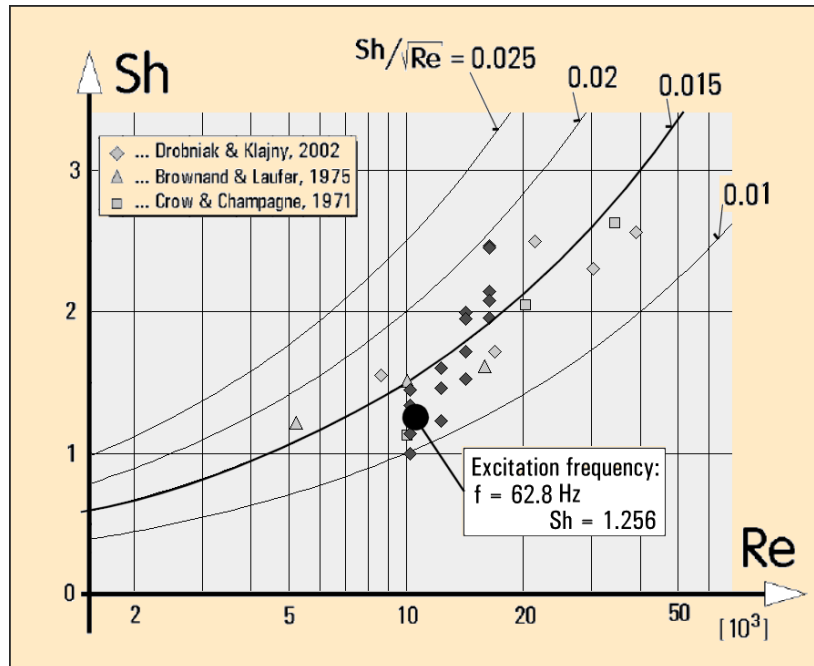
Fig. 14 Re-plotted data from the diagram shown in Fig. 3. Measured movement of the vortices in the sequence like the one in Fig. 7 indicate that the actual convection velocity of the vortex cores — with the result that the proper natural frequency (and hence the Strouhal number) should be considerably smaller than believed previously on the basis of Fig. 3. Indeed the re-plotting indicates a much better correspondence of our data from [4] with the values from references [10], [17], and [18].
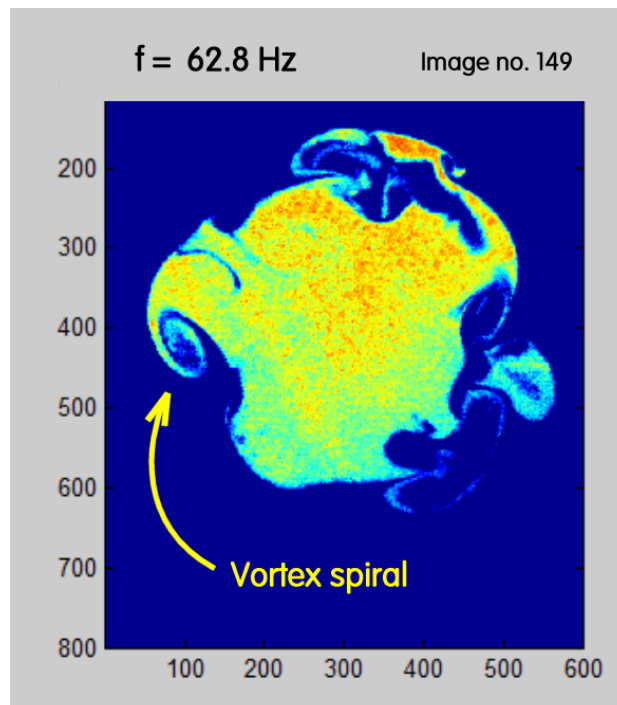
Fig. 15 A typical frame from the recorded video clip showing the jet cross section when excited at the lower frequency. Typical features occupying now the width of the mixing layer are now the vortex spirals.
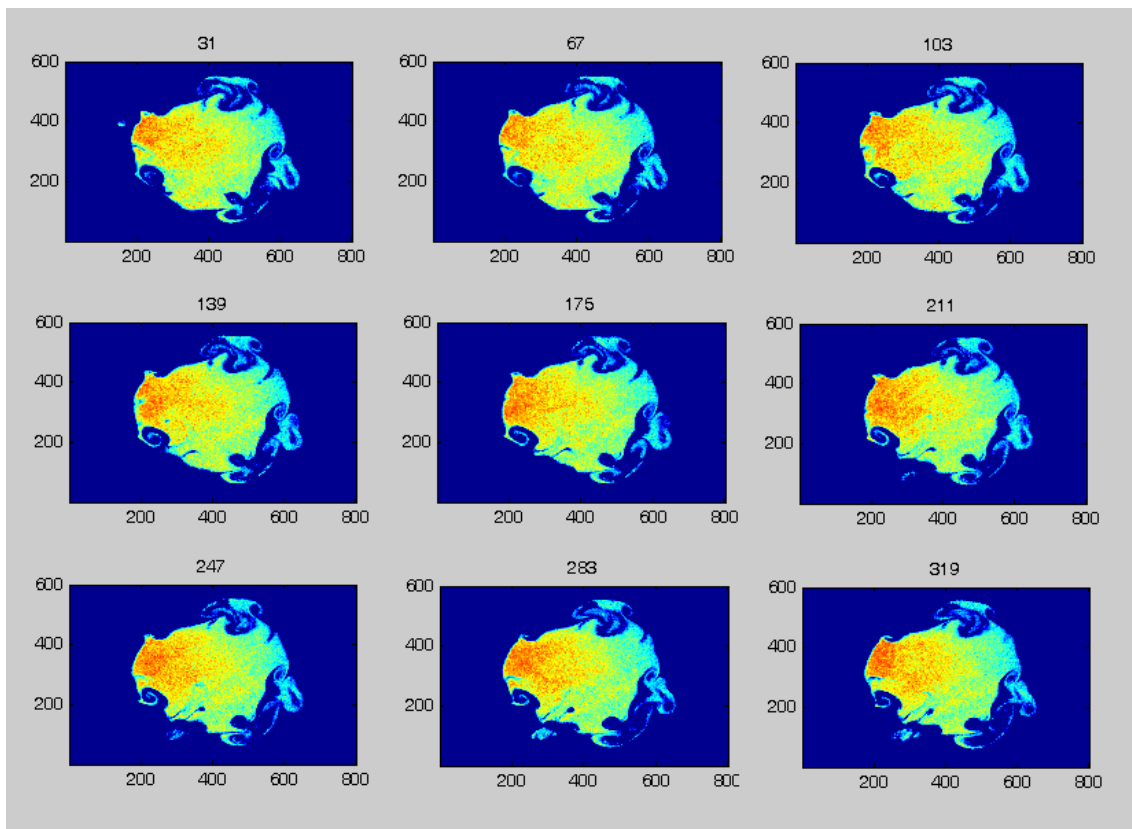
Fig. 16   An example of a sequence of the jet cross-section images taken at instants separated by the full period of the excitation (note the ordinal numbers of the images separated by increment 36). The shape is still rather irregular and the irregularity may seem to be chaotic, but the nearly exact repetition of the features at subsequent periods actually demonstrate a coherent character.

4. Questionable excitation frequency

The strange discrepancy between the expectations and observed flowfield images have led to search for explanation. The most obvious conclusion, that the complex character seen in the images was due to the effect of chaos caused by turbulence, was proved wrong by the remarkable similarity of the images taken at the same phase in different excitation periods (an example of this similarity is presented here in Fig. 16).

The obvious absence of large-scale object (large in relation to the jet diameter) indicated that the flowfield was probably broken into the small objects by too high applied excitation frequency – strangely enough, considering the quite good previous experience with fitting the conjectured shape of the vortex core, e.g. in Fig. 6. However, the image sequences like the one presented above in Fig. 7 made it now possible to evaluate rather exactly the convection velocity of the vortex cores – a paper on this subject is now in preparation by the first author. Indeed, the conclusion is that the proper natural frequency (and hence the Strouhal number) should be considerably smaller.

Inserting the new values into the same procedure as was the one used to evaluate Regunath's data in ref. [4] has now lead to a different diagram, replacing Fig. 3. This new version is presented here as Fig. 14.   Its credibility is certainly increased by the good agreement with the data from known references [10], [17], and [18].
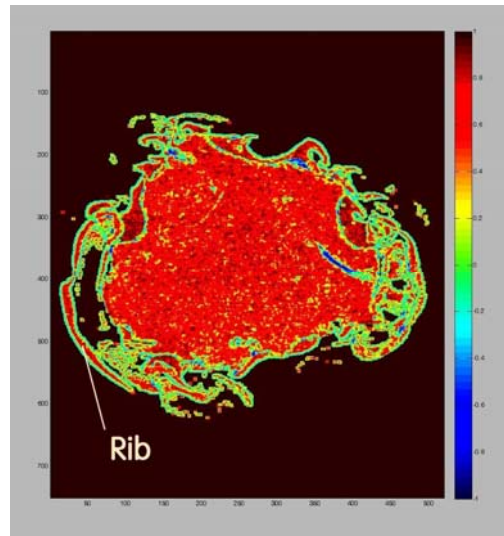
Fig. 17   Computed values of the correlation coefficient – with colour coding characterised by the colourbar at right. Red regions are steady, regions coloured green indicate chaotic turbulence. Blue regions that would indicate the moving – but shape-keeping – structures are not prominent here because the correlation was computed for image pair separated by only small time increment so that only narrow blue bands on the boundaries indicate the structure presence.

The flow visualisation experiments were then repeated with the new setting of the frequency. A typical result is presented in the example of the video-clip image in Fig. 15. Initially, no spectacular improvement was seen. There were, however, signs of the generated flow being nearer to what was expected. For example, in place of the not easily explained "voids" like A, B, and C in Figs. 11, 12 and 13, there are now seen spiralling objects – as indicated in Fig. 15 – of the character that could be expected in transversal sections through the helical vortex structures. Further processing of the images, such as the extraction of the correlation coefficient presented in Fig. 17, indicate what seems to be in an even better agreement with the expectation. It is the presence of the more or les stationary "ribs" on the outer edge of the mixing layer. In fact, some indication of the ribs is seen already in Fig. 15, at the right-hand top side. Even though the flowfield between the rib and the jet core shows considerable chaotic motions, it seems to be quite acceptable to fit the expected structures as passing through this space – as is indicated in Fig. 18.

Conclusions

Instead of providing explanation to the questionable features of the observations made earlier with the lateral sections through the impinging jet flowfields, the new transversal sections actually proved to be more enigmatic. A part of the explanation may be in the initially wrong choice of the triggering frequency with which the investigated structures were forced to appear. It now seems quite possible that the ribs that were found at the lower excitation frequency represent the outer part of the helical vortices. This is now the best explanation we can now provide for our observations. Additional experimental evidence will be, however, needed to support or repudiate this conjecture.

Acknowledgements
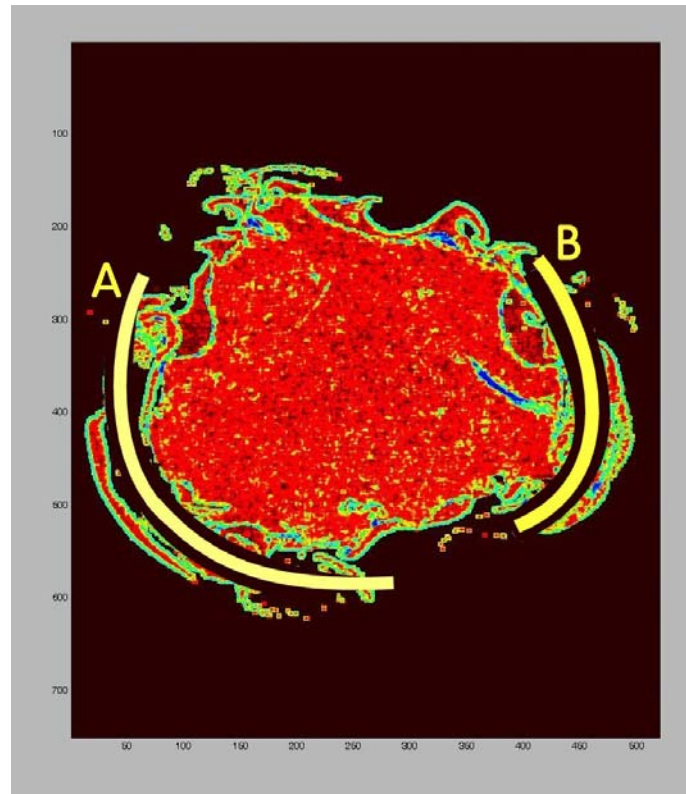
Fig. 18 The conjectured positions of the cores (thick yellow line) of the helical vortical structures. They full the width of the mixing-layer ring delineated by the "Ribs" from Fig.17.

References

[1]   Tesař V., Trávníček Z.: " *Increasing Heat and/or Mass Transfer Rates in Impinging Jets*", Joural of Visualization, ISSN 1343-8875, published by   The Visualisation Society of Japan, Vol. 8, No. 2, pp. 91-98, 2005

[2]   Hewakandamby B. N.: "*A numerical study of heat transfer performance of oscillatory impinging jets"*, International Journal of Heat and Mass Transfer Vol. 52, pp. 396–406, 2009

[3]   Tesař V.: "*Similarity Solutions of Jet Development Mixing Layers Using Algebraic and 1-equation Turbulence Models*", Acta Polytechnica - Journal of Advanced Engineering, ISSN 1210-2709, Vol.46, No.1,   pp. 40 - 56, 2006

[4]   Tesař V., Zimmerman W. B. J., Regunath G.: "*Helical Instability Structures in Swirling Jets*", Proc of the 8th International Symposium on Fluid Control, Measurements, and Visualization FLUCOME 2005, Chengdu, China, 2005

[5]   Trávníček Z., Kopecký V., Maršík F., Tesař V.**:** „*Bifurcated and Helical Impinging Jet Controlled by Azimuthally Arranged Synthetic Jets*", Proc. of HEFAT2007, 5th

International Conference on Heat Transfer, Fluid Mechanics and Thermodynamics, Paper TZ1; ISBN:978-1-86854-6435, Sun City, South Africa, July 2007.

[6] Tesař V., Něnička V., Šonský J., Kukačka L., Pavelka M.: "*Effect of Azimuthal Excitation in the Nozzle Exit on Structures Formed in Submerged Jets*", ISBN 978-80-87012-14-7; Proc. of Colloquium FLUID DYNAMICS 2008, Institute of Thermomechanics AS CR, v.v.i., Prague, October 2008

[7] Tesař V., Něnička V., Šonský J.: "*Extracting Information About Coherence in Jet Flows*", Proc of "ENGINEERING MECHANICS 2009", Conference with International Participation, ISBN: 978-80-86246-35-2, pp. 1333-1346, Svratka, May 2009

[8] Tesař V., Něnička V.: "*Phase-Synchornised Investigations of Triggered Vortices in Impinging Jets*", Proc of "ENGINEERING MECHANICS 2009", Conference with International Participation, ISBN: 978-80-86246-35-2, pp. 1321-1332, Svratka, May 2009

[9] Tesař V., Něnička V.: „*Study of Vortical Structures in Impinging Jets - New Methods and Approaches",* Proc. of ExHFT-7,   The 7th World Conference on Experimental Heat Transfer,Fluid Mechanics and Thermodynamics, Krakow, Poland, June-July 2009

[10] Drobniak S., Klajny R.: "*Coherent Structures in Axisymetric Free Jets*", Journal of Turbulence, Vol. 3, p. 1, 2002

[11] Regunath G., et al.: "*Experimental investigation and visualization of helical structures in a novel swirling jet*", Proc. of FEDSM06, ASME Joint U.S. – European Fluids Engineering Summer Meeting, Technical 32-5 Optical Methods 2, Miami, July 2006

[12] Regunath G.S., et al. : *"Experimental investigation of helicity in turbulent swirling jet using dual-plane dye laser PIV technique"*, Experiments in Fluids, ISSN 0723-4864, Springer Berlin/Heidelberg, Vol. 45, pp. 973-985, December 2008

[13] Tesař V.: "*The problem of off-axis transfer-effect extremes in impinging jets*", Proc. of XVIIth Internat. Scientific Conference of Depts. of Fluid Mechanics and Thermomechanics, p. 187, ISBN 80-88896-19-3, Herlany, Slovakia, June 1998

[14] Tesař V.: "*Characterisation of subsonic axisymmetric nozzles*", Chemical Engineering Research and Design, p. 1253, Volume 86, Issue 11, 2008

[15] Tesař V., Barker J.: "*Dominant vortices in impinging jet flows*", Journal of Visualisation, Japan, ISSN 1343-8875, Vol.5, No.2, p. 121, 2002

[16] Něnička V., et al. : "*Application of the Correlation Analysis to Identification of Coherent Structures in Free Plasma Flow*", Acta Technica CSAV, ISSN 0001-7043, Vol.. 48, Nr. 2, p. 175, 2003

[17] Crow S. C., Champagne F. H.: "*Orderly Structure in Jet Turbulence*", Journal of Fluid Mechanics, Vol. 8, part 3, p. 547, 1971

[18] Brownand F.K,. Laufer J.: "*The Role of Large Scale Structures in the Submerged Jets*," Trans. ASCE, p. 1571, 1975.

[19] Moiseev, S. S., et al.: „*Theory of generation of large-scale structures in hydrodynamic turbulence"*, JETP, 85, 1979-1987, 1983

[20] Moiseev S. S., Pungin V. G.: „*Analysis of Nonlinear Development of Helical Vortex Instability*", Fractals, Vol. 10, No. 4, p. 395, 2002